

Effect of Varied Control Technique in Modeling of Unbalanced Radial Distribution System

M Sai Balaji¹, P Sujatha²

¹EEE Department - JNTUA College Of Engineering,

² Professor, EEE Department - JNTUA College Of Engineering,

Abstract— Modeling of distribution system has got an importance in successful maintenance of a power system and in serving the demand optimally. A specific case related to distribution system viz., unbalanced radial distribution system has been taken up to model using dynamic phasors with Fuzzy logic based MPPT control in this paper. Comprehensively the model is analytical in nature and called as analytical model of an unbalanced radial distribution system consisting of a single-phase photo-voltaic (PV), a three-phase induction machine load, a three-phase power factor correction capacitor (PFC), and a load. The developed model with fuzzy logic control is better in performance represented in terms of THD with respect to the PI control. The fuzzy control integrated model is capable of small-signal analysis and can be used effectively to identify variety of stability and /or harmonic issues in distribution networks, (e.g. instability due to weak grid) in a better than other control techniques. The analytical model is built in Matlab where power electronic switching details are included. The comparative analysis between the varied control techniques viz., PI control and Fuzzy control is carried out by validating the THD values of I_{pv} of PV and V_{abc} of induction machine.

Keywords— Dynamic phasor (DP), Induction machine, Single- phase photovoltaic, Small-signal analysis, Fuzzy control MPPT

I. INTRODUCTION

Increased focus on reduction in pollution into environment by making world agreements on carbon emissions has increased the use of renewable energy resources extensively from the past decade. From 2000 to 2010 total capacity of grid connected PV systems has seen a growth from 300 MW to 21 GW respectively [10]. Higher efficient PV panels that are being supplied at economical prices and subsidies have boosted the integration of solar technology in modern power systems.

Induction machine was proved to be the major part of load component in distribution system. By modeling the unbalanced radial distribution system that includes PV system and induction machine using Dynamic Phasors can be used in small signal analysis and to predict instability due to weak grid [1].

The comparison of the four modeling methods, ABC, DQ0, DP-ABC and DPDQ0, in [11] illustrates the potential application of DPs in modeling the Electrical Power Systems for acceleration simulation studies, especially for the system under fault condition. With an increase in system complexity, the benefits from DPs will increase simultaneously.

The fuzzy logic based MPPT technique can track the maximum power point faster compare to the P&O based MPPT technique. It has the capability of reducing the voltage fluctuation after MPP has been recognized. The efficiency of the fuzzy logic controller in maintaining the stable maximum power point is studied in [8].

The pitfall of the DP model established in [1] is that it neglects the dynamics of MPPT technique of PV system. This paper argues that there is considerable amount of importance needed to be given for the above mentioned issue. An attempt has been done in this paper to emanate the importance of controlling technique of MPPT by analysing the percentage total harmonic distortion (%THD). In the following sections DP model of the system components has been understood and the better control technique model is suggested.

II. DYNAMIC PHASOR CONCEPT

Dynamic phasor (DP) models provide abundant merits, including: 1) the capability of small-signal analysis and 2) availability of large step size simulations. The main idea of DP comes from describing the waveform $x(\tau)$ on interval $[t - T, t]$ by Fourier Series [2]:

$$x(\tau) = \sum_{k=-\infty}^{\infty} X_k(t) e^{jk \omega_s t} \quad (1)$$

Where $\omega_s = 2\pi/T$ and X_k is the k th complex Fourier coefficient or DP. Due to the fact that these coefficients are constant at steady state, the DP model can be linearized for small-signal analysis. The k th DP of the time varying signal $x(\tau)$ can be obtained by (2) [2]:

$$X_k(t) = \frac{1}{T} \int_{t-T}^t x(\tau) e^{-jk\omega_s\tau} d\tau = \langle x \rangle_k(t) \quad (2)$$

Where $\langle \cdot \rangle_k$ denotes the k th harmonic DP.

The main characteristics of the DP modelling are described as follows [2]:

$$\left\{ \begin{array}{l} \langle \frac{dx}{dt} \rangle_k = \frac{dX_k}{dt} + jk\omega X_k \\ \langle x \cdot y \rangle_k = \sum_{l=-\infty}^{\infty} (X_{k-l} \cdot Y_l) \end{array} \right\} \quad (3)$$

Equation (3) describes the relationship between the DP of a derivative versus the DP of the original signal while (3) describes the relationship between the DP of a product versus the DPs of the individual variables. In this paper the DP model of a distribution system composed of a single-phase PV, a three-phase induction machine, a PFC and distribution lines represented by RL circuits [1] has been studied for improving the THD value by using a better controlling technique.

The DP models in the abc frame can be derived by converting the DP model from the positive-, negative-, and zero-sequence (pnz) reference frame [3]. The original signals in the abc frame can be expressed by pnz DPs as follows:

$$\begin{bmatrix} x_a \\ x_b \\ x_c \end{bmatrix}(\tau) = \sum_{l=-\infty}^{\infty} e^{jk\omega_s\tau} \frac{1}{\sqrt{3}} \begin{pmatrix} 1 & 1 & 1 \\ \alpha^* & \alpha & 1 \\ \alpha & \alpha^* & 1 \end{pmatrix} \begin{bmatrix} X_{p,l} \\ X_{n,l} \\ X_{z,l} \end{bmatrix} \quad (4)$$

Where l stands for the harmonic component index, M is the transformation matrix ($M^H = M^{-1}$) from pnz to abc . The relation of DPs of abc variables with the DPs of pnz sequences can be seen as follows:

$$\begin{bmatrix} X_{a,l} \\ X_{b,l} \\ X_{c,l} \end{bmatrix} = M \begin{bmatrix} X_{p,l} \\ X_{n,l} \\ X_{z,l} \end{bmatrix} \quad (5)$$

III. SYSTEM CONFIGURATION AND MODELING

The study system taken from [1] is shown in Fig. 1. The distributed system consists of a single-phase PV station installed in phase a of the system, a 3-phase induction machine, a 3-phase PFC, and a 3-phase load.

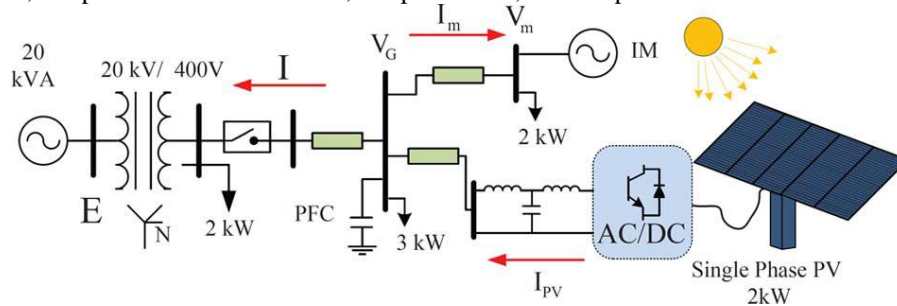


Fig. 1. Study system

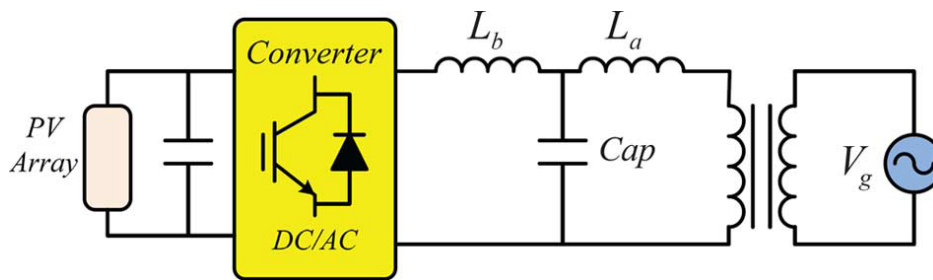


Fig. 2. Basic configuration of PV system.

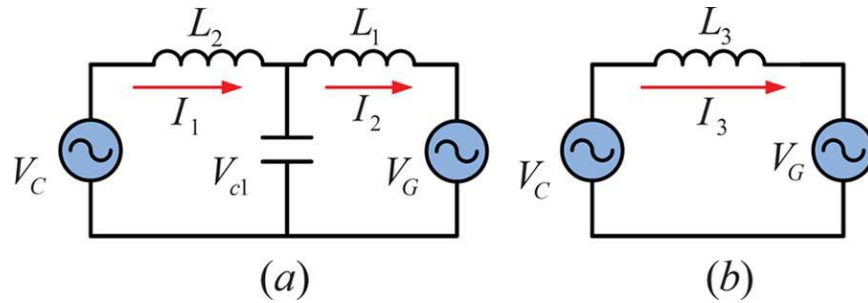


Fig. 3. Simplified PV model with different filters. (a) LCL filter (b) L filter

A. DP Model of a Single-Phase PV

Traditionally, two-stage converters (a DC-AC converter after a DC-DC converter) have been used for PV systems. Two-stage converters need additional devices compared with single-stage converters. Therefore, single-stage converters have been implemented in PV grid integration [4]–[7]. The basic configuration of a single-phase PV is illustrated in Fig. 2. The main elements of the single-stage PV are the proportional resonant (PR) current controller and the output filters.

Fig. 2 shows the basic configuration of an LCL filter in a single-phase PV. It is composed of two inductances and one capacitor connected to the grid through a single-phase transformer. The simplified model of PV connected to the grid with an L or an LCL filter has been illustrated in Fig. 3. The output voltage of the DC-AC converter is v_{con} , the filter inductances are L_a and L_b , and the grid side voltage is v_G . Note that the transformer can be represented by an inductor L_T . Therefore, $L_2 = L_b$ and $L_1 = L_a + L_T$. Furthermore, for a PV connected to an L filter, if L_f is used for the L filter inductance, $L_3 = L_f + L_T$.

The time-domain equations of the system for the LCL filter are as follows:

$$\begin{cases} L_1 \frac{di_1}{dt} = v_{c1} - v_G \\ L_2 \frac{di_2}{dt} = v_{con} - v_{c1} \\ C_1 \frac{dv_{c1}}{dt} = i_2 - i_1 \end{cases} \quad (6)$$

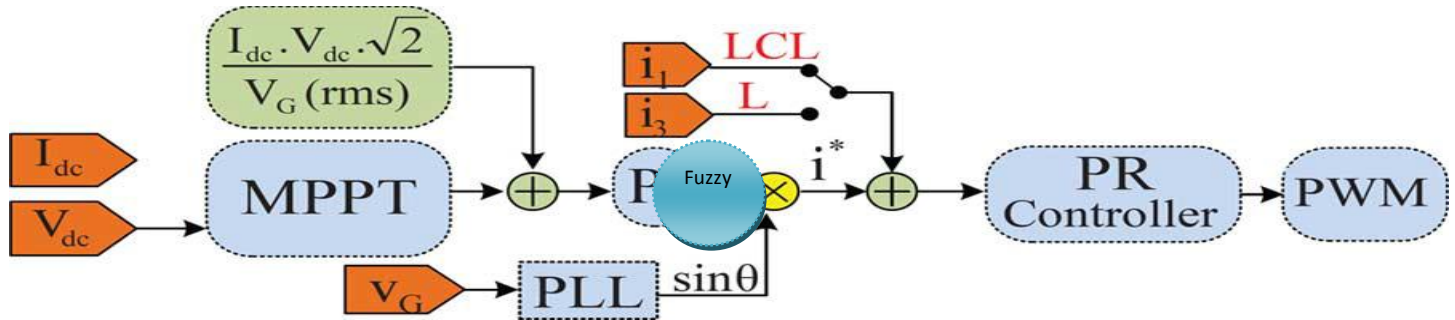


Fig. 4. Basic control of a single-phase PV.

The dynamics of the PV system with LCL filter in DP is expressed as follows. It should be noted that only the first harmonic is considered for the derivation of dynamic phasor coefficients [1]:

$$\begin{cases} I_1 = \frac{1}{L_1}(V_{c1} - V_G) - j\omega_s I_1 \\ I_2 = \frac{1}{L_2}(V_{con} - V_{c1}) - j\omega_s I_2 \\ V_{c1} = \frac{1}{C_1}(I_2 - I_1) - j\omega_s V_{c1} \end{cases} \quad (7)$$

It should be noted that is the DP of the output voltage of PV inverter. For an L filter enabled PV system, the basic DP equation of the PV system connected to grid is

$$I_3 = \frac{1}{L_3}(V_{con} - V_G) - j\omega_s I_3. \quad (8)$$

A detailed control block diagram of the single-stage single phase PV is illustrated in Fig. 4. It is composed of a maximum power point tracking (MPPT) unit, a proportional resonant (PR) controller, a phase-locked-loop (PLL), and a pulse width modulation (PMW) pulse generation unit. In this paper, the effect of PI control unit in MPPT unit has been taken into account before going to control unit an attempt has been made here to understand the DP models of PR controller and the LCL filter.

1) *DP Model of a PR Controller:* PR control is used to track ac signals. The PR controller in Fig. 4 tries to provide unity power factor power from the PV. Therefore, the current reference is synchronized with the grid voltage through a PLL. The dynamics of a PR controller considering only the fundamental harmonics can be expressed as

$$v_{con} = \left(K_p + \frac{K_r s}{s^2 + (\omega_s)^2} \right) (i^* - i_1)$$

$$= \left[K_p + K_r \left(\frac{0.5}{s + j\omega_s} + \frac{0.5}{s - j\omega_s} \right) \right] (i^* - i) \quad (9)$$

where i^* is the reference current comes from PV array. i_1 is the grid current when the PV enhanced with LCL filter. In a case where the PV is interconnected with an L filter, i_1 will be replaced by i_3 , which is the grid current. Defining intermediate state variables x_1 and x_2 , where

$$\begin{cases} (s + j\omega_s)x_1 = 0.5(i^* - i) \\ (s - j\omega_s)x_2 = 0.5(i^* - i) \end{cases} \quad (10)$$

Rewriting (10) in time domain gives (11):

$$\begin{cases} \frac{dx_1}{dt} + j\omega_s x_1 = 0.5(i^* - i) \\ \frac{dx_2}{dt} - j\omega_s x_2 = 0.5(i^* - i) \end{cases} \quad (11)$$

Applying the characteristics of DP, the DP relationship can be derived

$$\begin{cases} \frac{dX_1}{dt} = 0.5(I^* - I_1) - 2j\omega_s X_1 \\ \frac{dX_2}{dt} = 0.5(I^* - I_1) \end{cases} \quad (12)$$

The DP of the converter output voltage's fundamental frequency component can be expressed as

$$V_{con} = K_{p1}(I^* - I_1) + K_{r1}(X_1 + X_2). \quad (13)$$

2) *Maximum Power Point Tracking Controller:* Maximum power point tracking controller used in this paper is Fuzzy Logic Controller. Fuzzy logic control is a convenient way to map an input space to output space. Fuzzy logic uses fuzzy set theory, in which a variable is a member of one or more sets, with a specified degree of membership. Recently fuzzy logic controllers have been introduced in the tracking of the MPP in PV systems. They have the advantage to being robust and relatively simple to design as they do not require the knowledge of the exact model. They do require in the other hand the complete knowledge of the operation of the PV system by the designer [8]. Fig 5 shows the block diagram of Fuzzy Logic Controller.

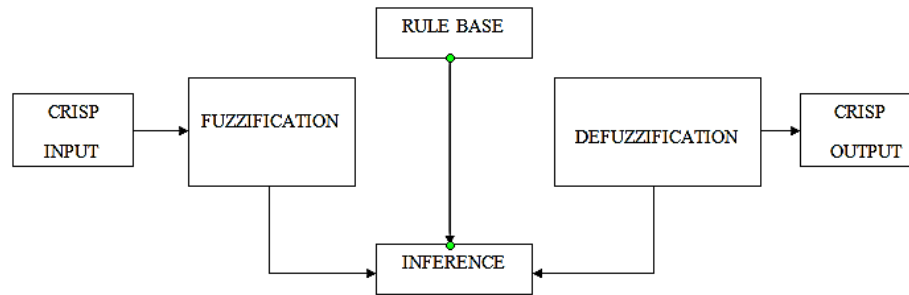


Fig 5: Block diagram of fuzzy logic controller

A fuzzy logic controller basically includes three blocks. They are fuzzification, inference and defuzzification. The fuzzy logic controller requires that each input/output variable which define the control surface be expressed in fuzzy set notations using linguistic levels. The process of converting input/output variable to linguistic levels is termed as Fuzzification. The

fuzzification method used in this model is triangular method. The behaviour of the control surface which relates the input and output variables of the system are governed by a set of rules. A typical rule would be–“If x is A THEN y is B” [8]. When all the rules are fired, the resulting control surface is expressed as a fuzzy set to represent the constraints output. This process is termed as inference. Defuzzification is the process of conversion of fuzzy quantity into crisp quantity. There are several methods available for defuzzification. The most commonly used is centroid method. The defuzzification method used in this paper is centroid method.

3) Fuzzy logic controller: Fuzzy logic is implemented to obtain the MPP operating voltage point faster and also it can minimize the voltage fluctuation after MPP has been recognized. The proposed fuzzy logic based MPPT controller has two inputs and one output. The error $E(k)$ and change in error $CE(k)$ are the input variables to Fuzzy Logic Controller and is given below in equation (14) & (15) for k th sample time [9] :

$$E(k) = \frac{dP}{dV} = \frac{[P_{pv}(k) - P_{pv}(k - 1)]}{[V_{pv}(k) - V_{pv}(k - 1)]} \quad (14)$$

$$CE(k) = E(k) - E(k - 1) \quad (15)$$

Where $P_{pv}(k)$ denotes the power of photovoltaic panel. The input variable $E(k)$ represents the error which is defined as the change in power with respect to the change in voltage. Another input variable $CE(k)$ expresses the change in error. The output of the Fuzzy Logic Controller is duty cycle (D) which should be given to the converter.

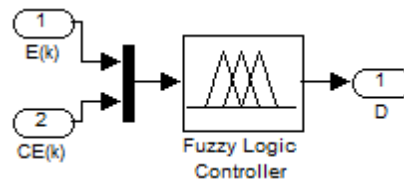


Fig 6: Fuzzy logic controller

Fig.6 represents the Fuzzy Logic Controller in which $E(k)$ and $CE(k)$ are the input variables and D as the output variable. To design the FLC variables which can represent the dynamic performance of the system to be controlled, should be chosen as the inputs to the controller. The input and output variables are converted into linguistic variables. In this case, five fuzzy subsets, NB (Negative Big), NS (Negative Small), ZE (Zero), PS (Positive Small) and PB (Positive Big) have been chosen.

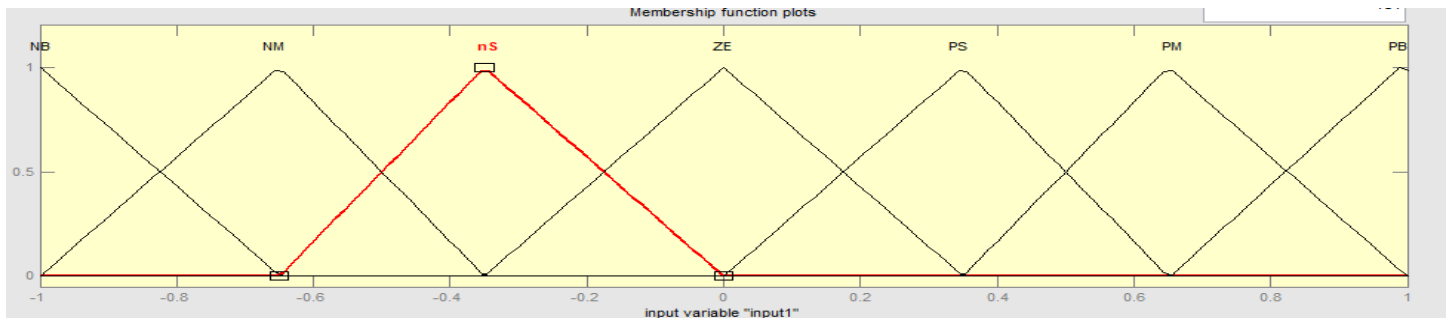


Fig 7 (a) Input 1 Error $E(k)$ noted as voltage V_{mpp}

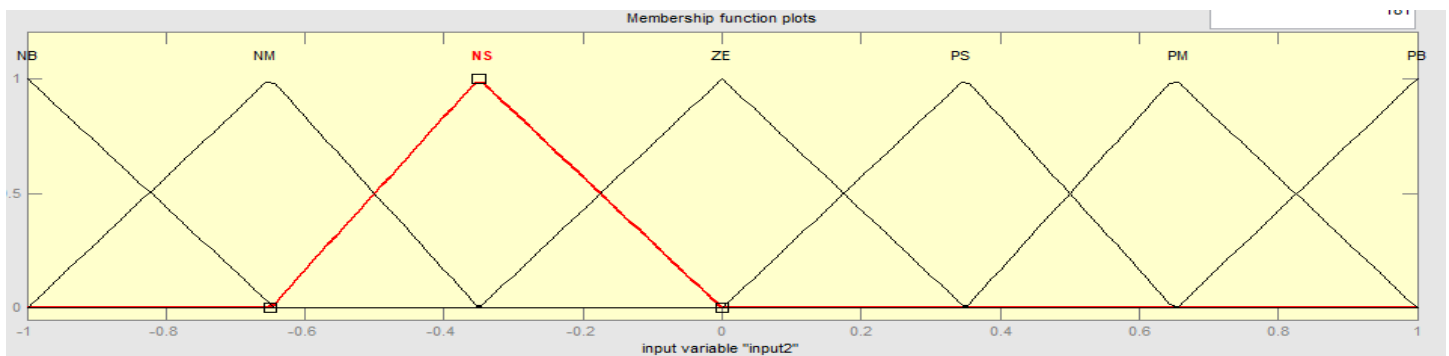


Fig 7 (b) Input 2 Change in Error $CE(k)$ noted as voltage dV_{mpp}

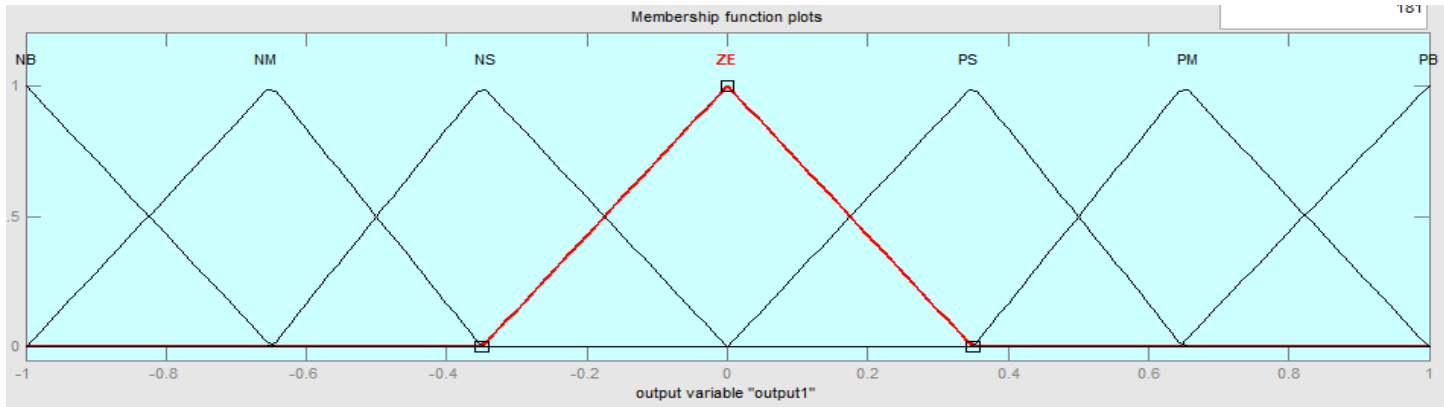


Fig: 7 (c) Control signal output of the Fuzzy controller

Table: 1. Fuzzy Rule Table

Error E(k)→	NB	NS	ZE	PS	PB
Change in error CE(k)↓					
NB	ZE	ZE	PB	PB	PB
NS	ZE	ZE	PS	PS	PS
ZE	PS	ZE	ZE	ZE	NS
PS	NS	NS	NS	ZE	ZE
PB	NS	NB	NB	ZE	ZE

The columns in table 1 is noted as error E(k) which is input variable 1 as shown in eq (14) and the rows in table 1 are change in error CE(k) noted from eq (15). The error and change in error are noted as variables V_{mpp} and dV_{mpp} which can be understood as maximum power point voltage and change in maximum power point voltage respectively.

B. DP Model of an Induction Machine

Since the single-phase PV will introduce unbalance in the distribution system, the induction machine will be modeled to include unbalance effect. Negative-sequence components in the stator voltage can cause a clockwise rotating stator flux. When this flux is interacting with the counter-clockwise rotating rotor flux, a 120-Hz torque ripple will appear. In turn, the rotating speed will have ripples with 120-Hz frequency. To count in the negative effect, the dynamic model of a three-phase induction machine in [3] based on *pnz*-sequence of components is adopted in the paper [1] has been studied. The space-vector model of a squirrel-cage induction machine with magnetic saturation and slot harmonics neglected is presented as follows:

$$\left\{ \begin{array}{l} \vec{v}_s = \left(r_s + L_s \frac{d}{dt} \right) \vec{i}_s + L_m \frac{d}{dt} \vec{i}_r \\ 0 = L_m \frac{d}{dt} \vec{i}_s + \left(r_r + L_r \frac{d}{dt} \right) \vec{i}_r - j\omega_r \frac{P}{2} (L_m \vec{i}_s + L_r \vec{i}_r) \\ J \frac{d}{dt} \omega_r = \frac{3P}{4} L_m \Im(\vec{i}_s \vec{i}_s^*) - B\omega_r - T_L \end{array} \right. \quad (16)$$

where $\vec{v}_s, \vec{i}_s, \vec{i}_r$ denote the stator voltage, stator current, and rotor current, respectively. T_L is the mechanical torque and ω_r is the rotor speeds and denote the stator and rotor quantities, respectively. \Im denotes the imaginary part. The DP model of an induction machine can be derived by considering the positive+ and negative-sequence components in stator/rotor voltages and currents, as well as the dc and the 120 Hz components in the rotating speed [3].

$$\begin{aligned}
 V_{ps} &= \left(r_s + j\omega_s L_s + L_s \frac{d}{dt} \right) I_{ps} + \left(j\omega_s L_m + L_m \frac{d}{dt} \right) I_{pr} \\
 0 &= \left(j\omega_s L_m + L_m \frac{d}{dt} \right) I_{ps} + \left(r_r + j\omega_s L_r + L_r \frac{d}{dt} \right) I_{pr} - j\omega_{r0} \frac{P}{2} (L_m I_{ps} + L_r I_{pr}) - j\omega_{r2} \frac{P}{2} (L_m I_{ns}^* + L_r I_{pr}^*) \\
 V_{ns}^* &= \left(r_s - j\omega_s L_s + L_s \frac{d}{dt} \right) I_{ns}^* - \left(j\omega_s L_m - L_m \frac{d}{dt} \right) I_{nr}^* \\
 0 &= \left(L_m \frac{d}{dt} - j\omega_s L_m \right) I_{ns}^* + \left(r_r - j\omega_s L_r + L_r \frac{d}{dt} \right) I_{nr}^* - j\omega_{r0} \frac{P}{2} (L_m I_{ns}^* + L_r I_{nr}^*) - j\omega_{r2} \frac{P}{2} (L_m I_{ps} + L_r I_{pr}) \\
 J \frac{d}{dt} \omega_{r0} &= \frac{2P}{4} L_m \Im(I_{ps} I_{pr}^* + I_{ns}^* I_{nr}) - B\omega_{r0} - T_L \\
 J \frac{d}{dt} \omega_{r2} &= \frac{2P}{8} L_m \Im(I_{ps} I_{nr} + I_{ns} I_{nr}) - (B + j2J\omega_s) \omega_{r2} \tag{17}
 \end{aligned}$$

where the subscripts p and n stand for positive and negative sequence components, respectively.

Since the DP model for the PV system is based on phase a , to integrate the induction machine model with the PV system model, the above pnz model will be converted from and to the abc frame using the relationship presented in eq.(5). The block diagram of the conversion has been illustrated in Fig. 8

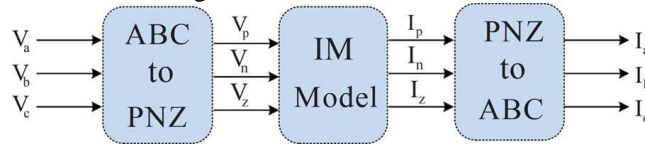


Fig.8 Conversion from abc to pnz and back to abc for an induction machine.

C. PFC and the Integrated System

Considering that there is a three-phase PFC in parallel with the PV, the circuit model of the distribution system can be illustrated

as in Fig. 9, where C denotes the capacitance of the PFC, I_m is the induction machine's stator current, I is the line current, R and L are the distribution line's parameters, R_L is the load model, and E is the system voltage.

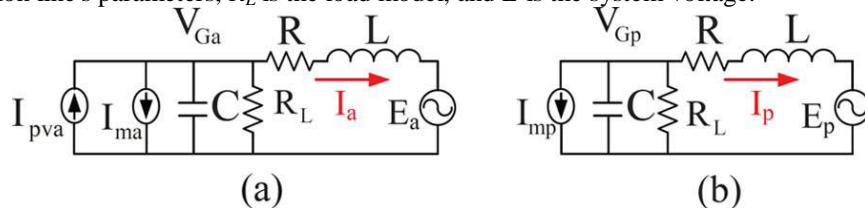


Fig. 9 (a) Circuit model of the distribution system with PV in phase a. (b) Circuit model of the distribution system in phase b and c

For phase a , the DP model of the integrated system can be expressed as

$$\left\{ \begin{aligned} \frac{d}{dt} I_a &= \frac{1}{L} (-j\omega_s L + R) I_a + V_{Ga} - E_a \\ \frac{d}{dt} V_{Ga} &= \frac{1}{C} \left(- \left(j\omega_s C + \frac{1}{R_L} \right) V_{Ga} - I_{ma} + I_{PV} - I_a \right) \end{aligned} \right\} \tag{18}$$

where two state variables (grid voltage and grid current) have been introduced.

For phase b and c , the DP model of the integrated system can be expressed as

$$\left\{ \begin{aligned} \frac{d}{dt} I_p &= \frac{1}{L} (-j\omega_s L + R) I_p + V_{Gp} - E_p \\ \frac{d}{dt} V_{Gp} &= \frac{1}{C} \left(- \left(j\omega_s C + \frac{1}{R_L} \right) V_{Gp} - I_{mp} - I_p \right) \end{aligned} \right\} \tag{19}$$

Where p represents either phase b or phase c .

The individual elements such as PV systems, induction machine loads and resistive loads are modeled as current sources or passive elements. Through the PFC dynamics and the grid inductor dynamics, the individual current sources are then

integrated with the grid voltage. As long as the distribution system is radial, additional unbalanced elements can be modeled as shunt current sources or passive elements and easily integrated into the overall system model [1].

IV. CASE STUDIES

The analytical model for the entire distribution system derived in paper [1] has been investigated in Section III. The dynamics of MPPT was neglected for simplicity in paper [1]. An effort has been made to measure the neglected effect of MPPT in the DP model presented in [1]. The said effort is carried out by constructing the physical model of the study system taken from [1] with both PI control and Fuzzy control separately. And the total harmonic distortion THD in PV current I_{pv} and voltage of induction machine V_{abc} of both models with PI control and Fuzzy control has been analysed. The model has been built in Matlab/Simulink based on the physical circuit connection.

Three case studies have been carried out.

- In the *first* case, the analytical model in Simulink with PI control is benchmarked with the high-fidelity model with Fuzzy control in Simulink. Dynamic simulation results are compared for the same dynamic event: a step change in load torque of the induction machine.
- In the *second* case, the effect of unbalance on the dynamic performance is investigated by applying a ramp change in irradiance of the PV. This dynamic event matches with the cloud effect on a PV and a distribution system.
- In the *third* case, the effect of the grid-line length on stability is investigated.

The simulation results of different quantities with Fuzzy and PI in three case studies was presented as follows:

A. Case Study 1

In this part, the Matlab model-based simulation results with PI control are compared with the Matlab model-based simulation results with Fuzzy control. A single-phase PV is connected to the phase *a* of the system at the point of common coupling (PCC) shown as in Fig. 1. At $t = 4$ s, the induction machine's mechanical torque was applied a step change from 28 N.M to 23 N.M.

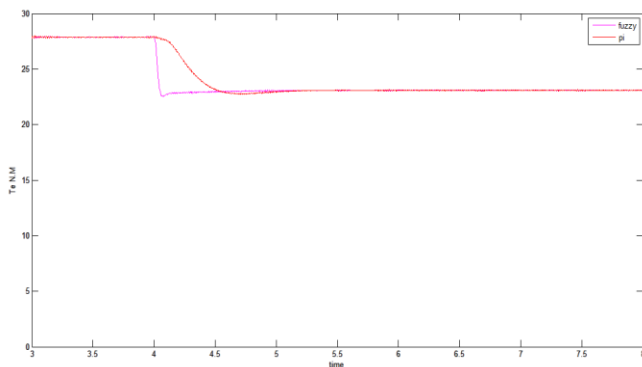


Fig: 10 Simulation results of Torque of Induction Machine

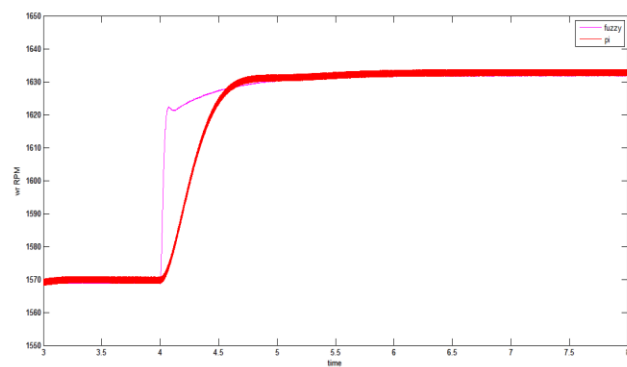


Fig: 11 Simulation results of Rotor Speed of Induction Machine

The simulation results of the electromagnetic torque and the rotor speed of the induction machine have been presented in Fig. 10 and Fig. 11 respectively. The difference in the dynamic response from the two varied control technique models can be observed well. In fig 10 torque decreased from 28 N-m to 23 N-m, with PI control the change was steep that implies a larger steady state error whereas with fuzzy control the change was sudden and step in nature. The PI and Fuzzy labels were mentioned in the top right of the figure 10.

In fig 11 rotor speed of the induction machine was raised from 1570 RPM to 1620 RPM with step change, then to 1630 RPM with a knee shape change with Fuzzy control. With PI control the rotor speed raised from 1570 RPM to 1630 RPM directly with lesser knee curve than Fuzzy control.

The simulation results for the line current, the line voltage and the PV current are presented in Fig. 12, Fig. 13 and Fig. 14 respectively. The results of the line current and the line voltage from both models can be observed well, which demonstrates the accuracy of the Fuzzy control model over PI control model suggested in this paper.

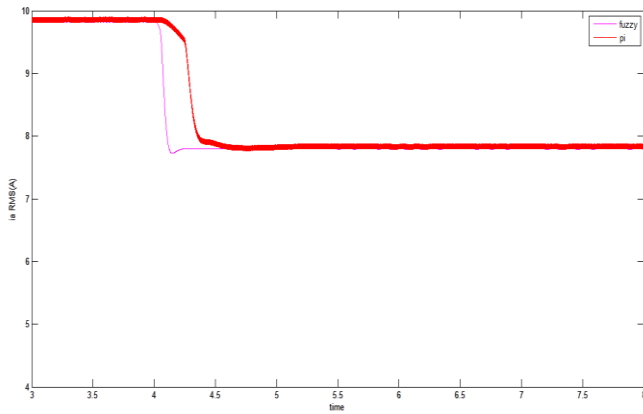


Fig: 12 Simulation results of stator current of Induction Machine

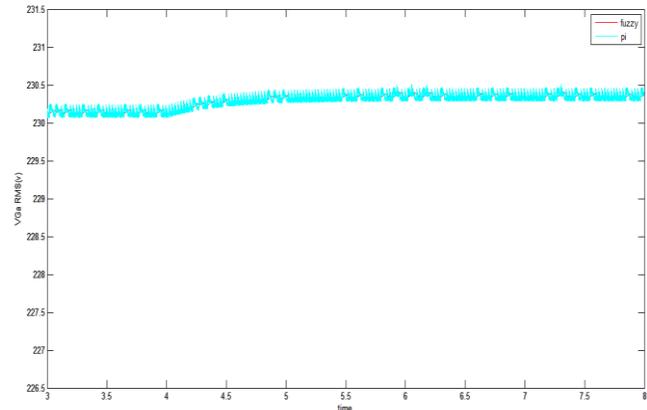


Fig: 13 Simulation results of stator voltage of Induction Machine

In fig 12 stator current of the induction machine dropped from 9.7 A to 7.8 A at $t=4$ seconds exactly with fuzzy control whereas with the PI control the stator current is prolonged upto 4.5 seconds from 4 seconds in the form of a steep curve and merged with the fuzzy control stator current at $t=5$ seconds.

In fig 13 the stator voltage of the induction machine has negligible variation from 230 V to 230.5 V. The simulation results of stator voltage with a change in torque from 28 N.M to 23 N.M with fuzzy control and PI control are fall in line with each other.

The PV power is constant and V_G has negligible variation; therefore the PV current of the analytical model is almost constant. This can be observed from the fig 14, the value of PV current I_{pv} stood at 8.9 A throughout the time period of 8 seconds. Also the simulation results of PV current for the effect of torque change with Fuzzy control and PI control fall in line with each other as shown in fig. 14.

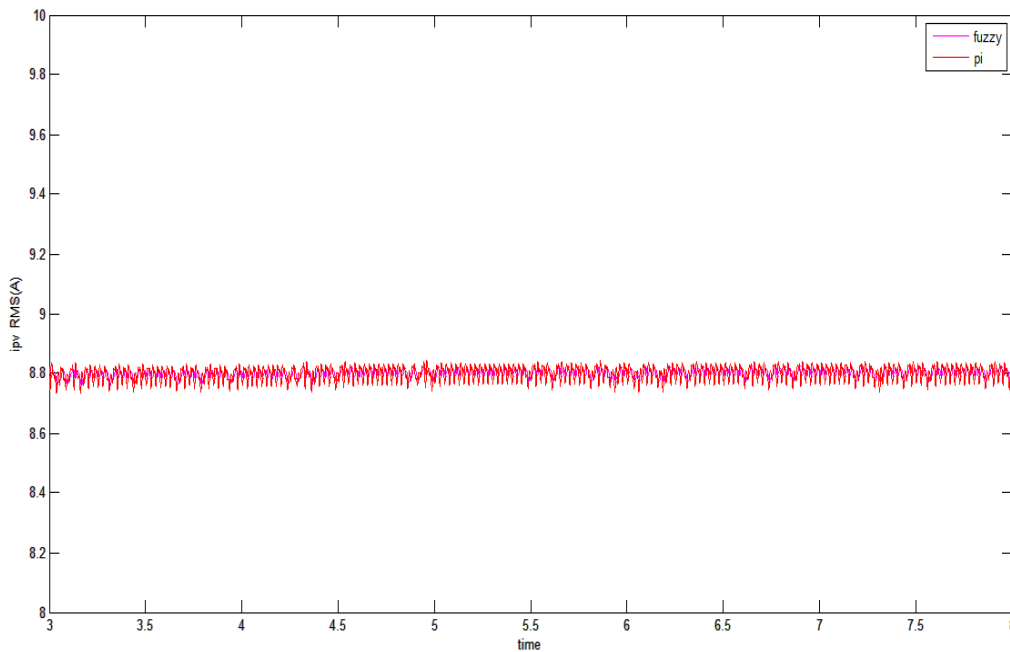


Fig: 14 Simulation results of PV current due to a step change in mechanical torque (from 28N.M to 23 N.M)

B. Case Study 2

- 1) *PV Irradiance Change:* In this part, the effect of PV irradiance change with fuzzy control model and PI control model will be simulated in Matlab/Simulink.

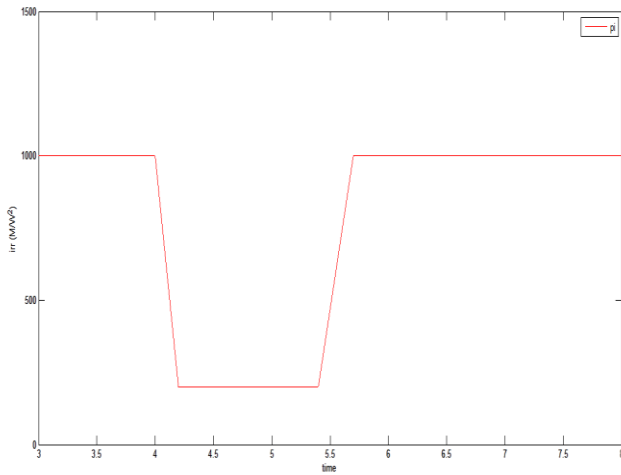


Fig: 15 Irradiance input to the PV panel

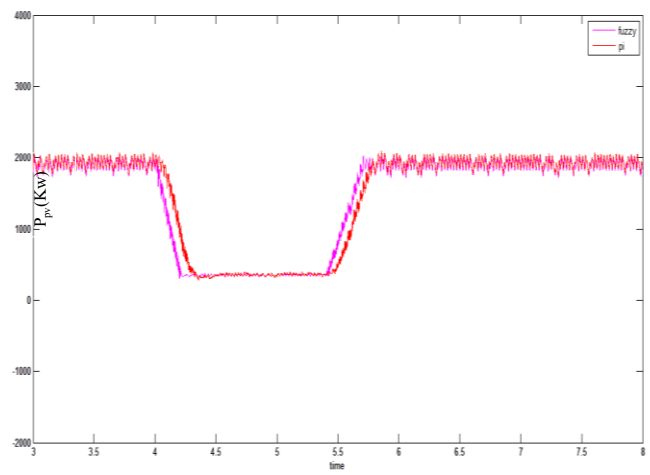


Fig: 16 Simulation results of PV Power (watt) for the effect of Irradiance change

In fig 15 the PV irradiance was set to 1000 W/M^2 previously. A ramp change will be applied at $t = 4\text{s}$ to decrease the irradiance to 200 W/M^2 in 0.2 s. Then after 1.4 s, the irradiance will be set back to 1000 W/M^2 .

The change of irradiance has been illustrated in detail in Fig. 15. The PV power which follows the irradiance order can be seen in Fig. 16. The PV power of the analytical model is set to follow the change of the irradiance. It can be noticed that the maximum power level (2 kW) is obtained when the irradiance is set to 1000 W/M^2 . The difference between the dynamics of Fuzzy control and PI control can be seen in fig 16 that the fuzzy control reaches the maximum value 2kw after irradiance been raised to 1000 W/M^2 slightly before the PI control reaches the value.

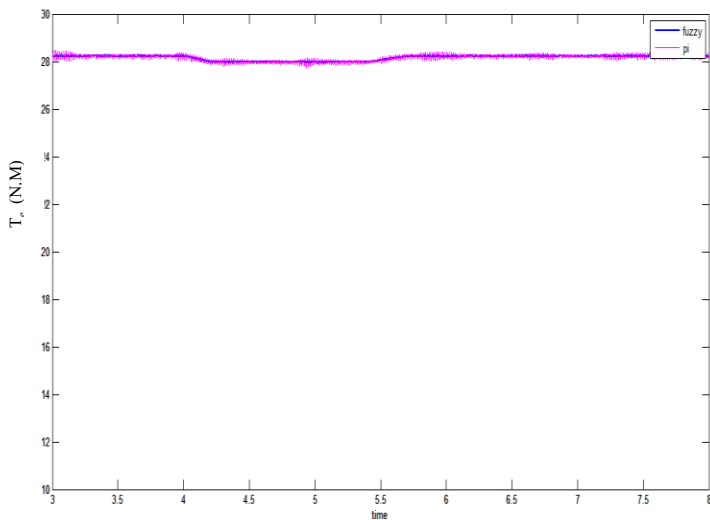


Fig: 17 Simulation results of Torque of Induction Machine for the effect of Irradiance change

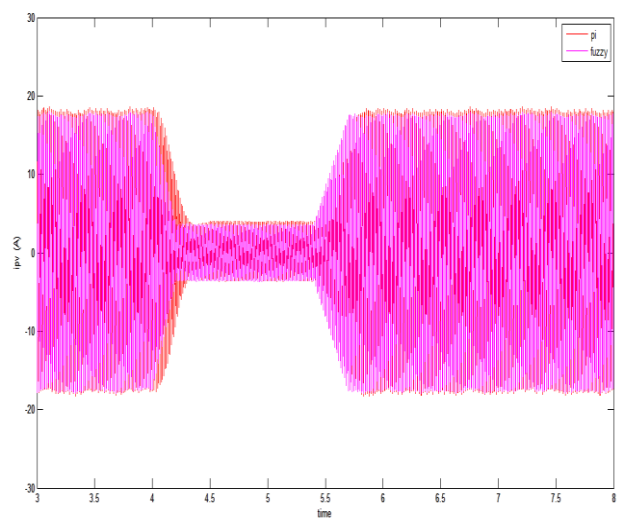


Fig: 18 Simulation results of PV current for the effect of irradiance change

Fig. 17 shows the electrical torque of the induction machine. When the irradiance is decreased due to clouds, the PV power is decreased, which leads to the decrease in the unbalance injection level to the system. The magnitude of the 120-Hz ripple has been decreased during the interval of 4 to 6 seconds. Fig. 17 shows the PV current which has been decreased due to the irradiance change from 4 to 6 seconds. In fig 17 the torque of induction machine with both Fuzzy control and PI control have shown the similar behavior and fall in line with each other.

In fig. 18 PV current for the irradiance effect with both Fuzzy control and PI control has been shown. There has been no hostile behavior between the two control models, the only difference that can be observed from fig. 18 is that Fuzzy control model converges more than the PI control model.

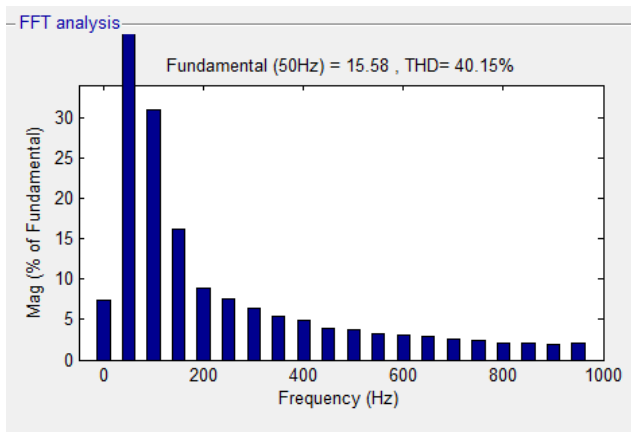


Fig 19: %THD of PV current with PI control for irradiance change

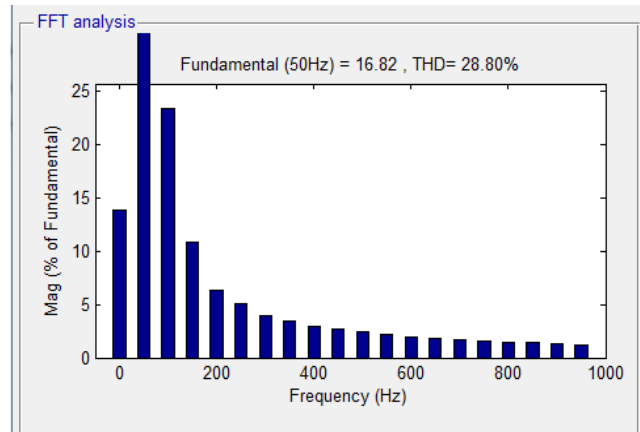


Fig 20: %THD of PV current with Fuzzy control for irradiance change

FFT analysis has been carried out for the PV current with PI control model and THD is shown in fig. 19. The THD value for the PV current with PI control for the effect of irradiance change is 40.15%. FFT analysis has been carried out for the PV current with Fuzzy control model and THD is shown in fig. 20. The THD value for the PV current with Fuzzy control for the effect of irradiance change is 28.80%.

C. Case Study 3

In Case 3, impact of line length on system stability was investigated by both PI control and Fuzzy control in Matlab/Simulink. The grid line length has been changed from 3 km to 15 km in order to observe its effect on dynamics. It is worth mentioning that increasing the line length more than 15 km causes non-convergence of the sweeping method for initialization. Therefore the results are only shown for the initial conditions where the system is able to converge.

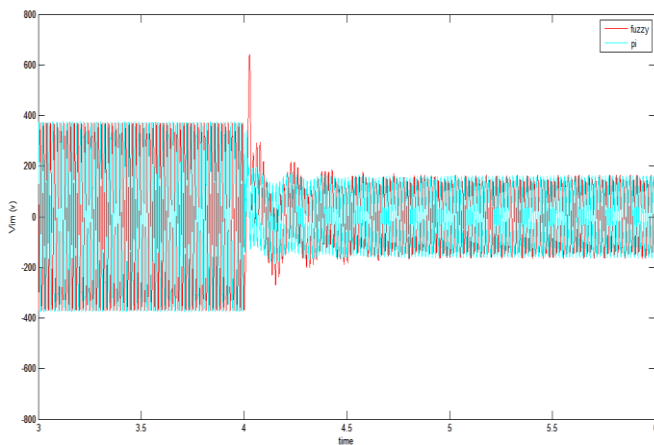


Fig 21: Simulation results of Stator Voltage of IM for the effect of grid line length increase

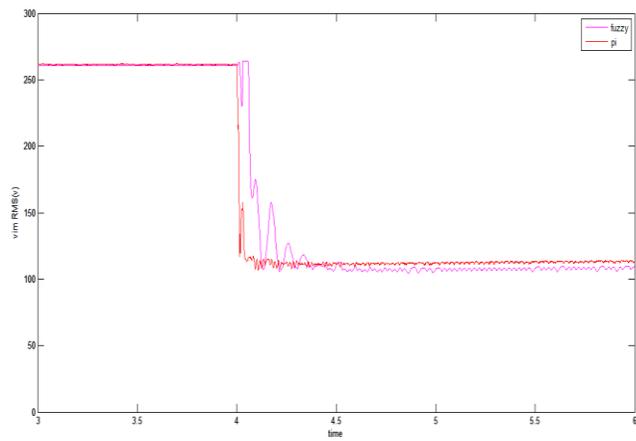


Fig 22: RMS stator voltage of IM for the effect of grid line length increase

In time-domain simulations, a dynamic event to increase the grid line from 3 km to 30 km was triggered. Initially the grid connection consists of two parallel lines. At $t = 4s$, a breaker of one line is opened so the effective line impedance increases suddenly. The stator voltage of the induction machine decreases significantly as shown in Fig. 21. Fig. 22 presents the dynamic response of the RMS value from 3.5 s to 6 s, which clearly shows the decline of the voltage magnitude.

In fig. 21 the stator voltage of the induction machine for the effect of the grid line length increase is shown, at $t=4$ seconds a breaker of one line is opened that decreases the voltage passes through a transient state between 4 to 4.3 seconds and settles down after 4.5 seconds. With PI control the voltage spike can be seen at $t=4$ seconds from fig. 21 whereas the voltage with Fuzzy control model decreases steadily from 4 seconds to 4.3 seconds after which fall in line with the voltage of PI control model.

In fig. 22 contrast behavior of the fuzzy with the proposed behavior has been seen. The RMS stator voltage of induction machine for the grid line length increase with PI control has shown better transient behavior than RMS stator voltage with Fuzzy control model after opening of a breaker of one line at $t=4$ seconds.

Due to the decrease of the stator voltage and system voltage magnitude, for the induction machine, its electromagnetic torque will decrease and its rotor speed will decrease as shown in Fig.23 and Fig.24. For the PV, since the reference power is kept intact, the reference current increases due to the decrease of the voltage. In turn, the PV current's magnitude increases as shown in Fig. 25. The entire system becomes unstable.

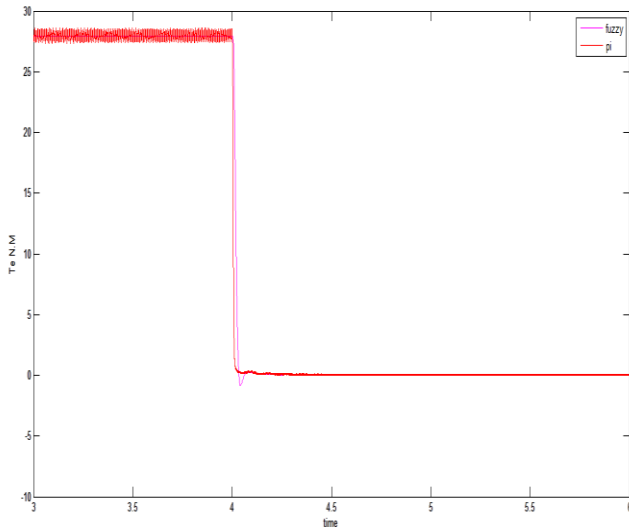


Fig 23: Simulation results of torque for the effect of grid line length increase

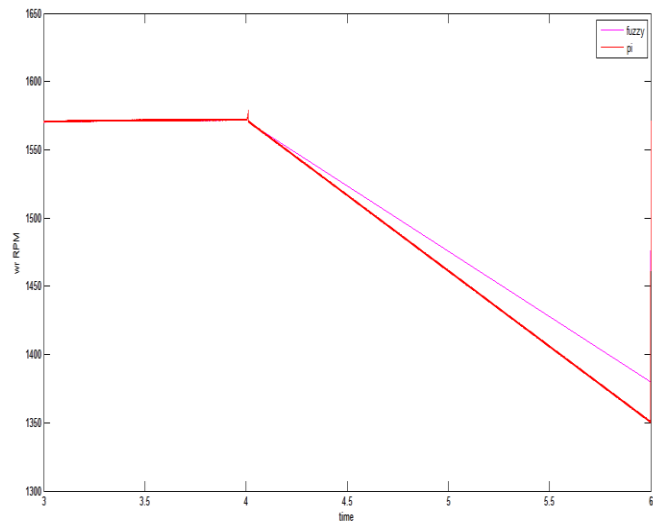


Fig 24: Simulation results of rotating speed for the effect of grid line length increase

The simulation results of torque for the effect of grid line length increase with PI control model and Fuzzy control model fall in line with each other and torque with Fuzzy control decreases beyond 0 value for fraction of milli-seconds after which falls in line with the torque of PI control model as shown in fig. 23.

The simulation results of the rotating speed for the effect of grid line length increase with PI control model and Fuzzy control model fall in line up to $t=4$ seconds after which the rotating speed with both control models undergoes a steep linear decrease. The rotating speed with Fuzzy control model exhibits a better behavior than the rotating speed with PI control. With increase in time period the difference between the two signals increase, it has been shown up to 6 seconds in fig. 24.

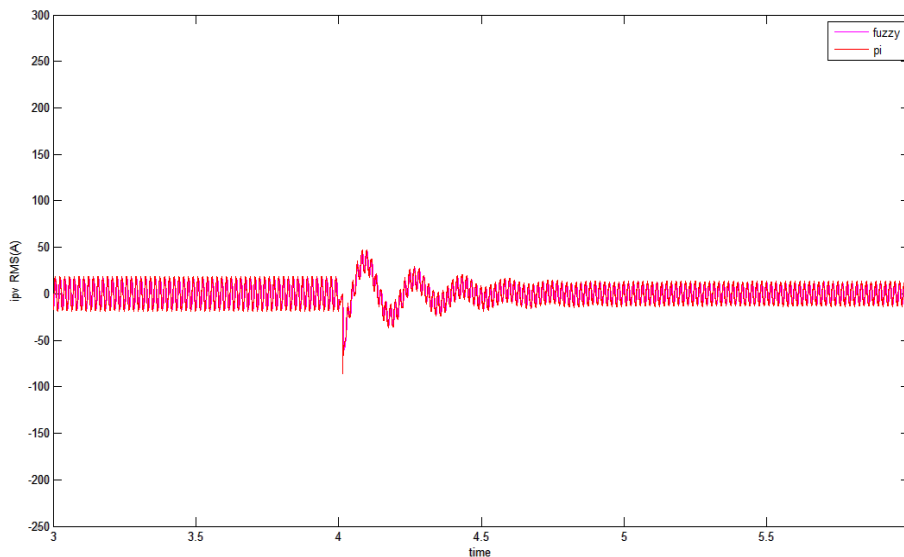


Fig:25 Simulation results of PV Current for the effect of grid line length increase

The simulation results of PV current for the effect of grid line length increase with Fuzzy control and PI control fall in line with each other as shown in fig. 25.

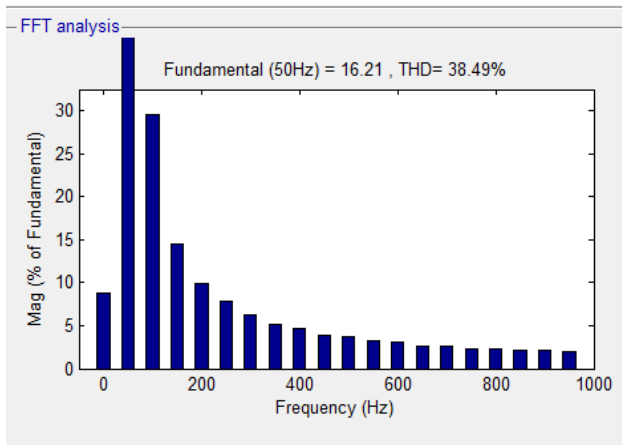


Fig: 26 a. %THD of PV current (38.49%) with PI control

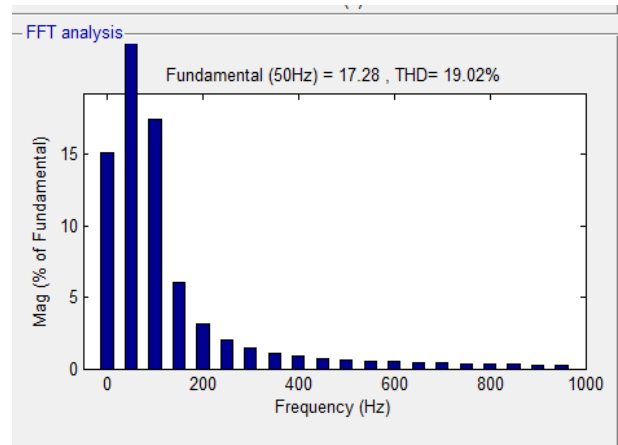


Fig.26 b. %THD of PV current (19.02%) with Fuzzy Control

Fig. 26(a) shows the total harmonic distortion THD of PV current with PI control which reads 38.49%. Whereas the total harmonic distortion THD value of PV current with Fuzzy control is 19.02% as shown in fig.26 (b).

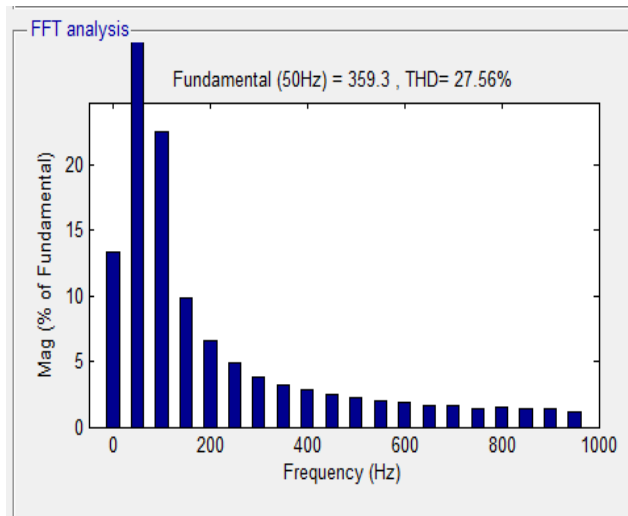


Fig: 27 a. %THD of Stator Voltage of IM (27.56%) with PI control

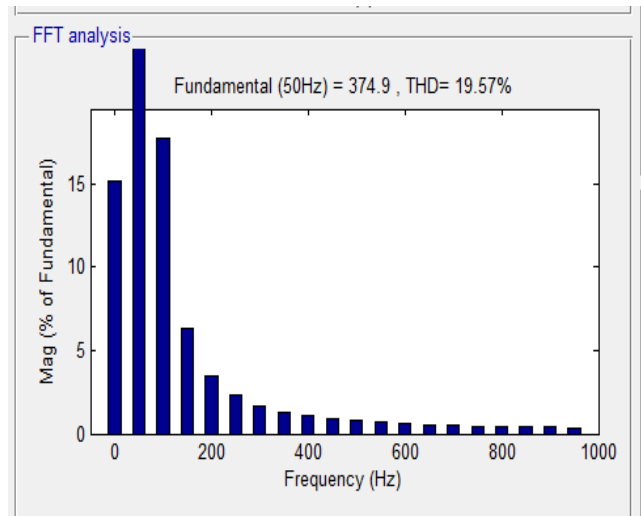


Fig: 27 b. %THD of Stator Voltage of IM (19.57%) with Fuzzy control

Fig 27(a) shows the total harmonic distortion THD value of Stator Voltage of Induction machine with PI control which reads 27.56%. whereas the total harmonic distortion THD value of Stator Voltage of Induction machine with Fuzzy control is 19.57% as shown in Fig 27(b).

V. CONCLUSION

In this paper, the effect of varied control techniques in a dynamic phasor-based model was investigated for an unbalanced radial distribution system consisting of a single-phase PV, a three-phase induction machine and a three-phase power factor correction capacitor with three case studies. The simulation results of different quantities in three case studies with Fuzzy control model have shown better behavior than PI control model except in case study 3 for stator RMS voltage of induction machine.

The difference in the THD values of PV current and Stator voltage with PI and Fuzzy control can be summarized and clearly understood by tabulating all the values obtained from the constructed models as shown in Table 2.

Table: 2. THD comparison values of PV current and Stator Voltage with PI and Fuzzy Control Techniques

Case Study	Parameter	%THD with PI control	%THD with Fuzzy control
2	i_{pv}	40.15	28.80
3	i_{pv}	38.49	19.02
3	V_{abc}	27.56	19.57

Table 2 shows the values of THD for PV current i_{pv} , stator voltage of induction machine V_{abc} with PI control and Fuzzy control. Percentage THD value of PV current i_{pv} for case study 2 with PI control is 40.15% and with fuzzy control is 28.80%. Percentage THD value of PV current i_{pv} with fuzzy control is reduced to 19.02 % from 38.49 % with PI control as shown in the table 2. THD value of stator voltage of induction machine with fuzzy control is reduced to 19.57% from 27.56% with PI control. From the discussion it is evident that fuzzy is the better control technique than PI and dynamic phasor modeling becomes more efficient with fuzzy control.

References

- [1] Dynamic Phasor-Based Modeling of Unbalanced Radial Distribution Systems by Zhixin Miao, Lakshan Piyasinghe, Javad Khazaei, Lingling Fan. *IEEE Transactions on Power Systems* (Volume: 30, Issue: 6, Nov. 2015)
- [2] A. M. Stankovic, B. C. Lesieutre, and T. Aydin, "Modeling and analysis of single-phase induction machines with dynamic phasors," *IEEE Trans. Power Syst.*, vol. 14, no. 1, pp. 9–14, Feb. 1999.
- [3] A. M. Stankovic, S. R. Sanders, and T. Aydin, "Dynamic phasors in modeling and analysis of unbalanced polyphase ac machines," *IEEE Trans. Energy Convers.*, vol. 17, no. 1, pp. 107–113, Mar. 2002.
- [4] M. Ciobotaru, R. Teodorescu, and F. Blaabjerg, "Control of single- stage single-phase PV inverter," in *Proc. IEEE Eur. Conf. on Power Electronics and Applicat.*, 2005, p. 10.
- [5] C. Meza, J. J. Negroni, D. Biel, and F. Guinjoan, "Energy-balance modeling and discrete control for single-phase grid-connected PV central inverters," *IEEE Trans. Ind. Electron.*, vol. 55, no. 7, pp. 2734–2743, 2008.
- [6] Y. Yang, K. Zhou, and F. Blaabjerg, "Harmonics suppression for single-phase grid-connected photovoltaic systems in different operation modes," in *Proc. Appl. Power Electronics Conf. Expo.*, 2013.
- [7] Y. Wang, P. Zhang, W. Li, W. Xiao, and A. Abdollahi, "Online over-voltage prevention control of photovoltaic generators in microgrids," *IEEE Trans. Smart Grid*, vol. 3, no. 4, pp. 2071–2078, Dec. 2012.
- [8] S. Karthika ,Dr. P. Rathika, Dr. D. Devaraj, "Fuzzy Logic Based Maximum Power Point Tracking Designed for 10kW Solar Photovoltaic System", *International Journal of Computer Science and Management Research*, Vol 2 Issue 2 February 2013.
- [9] C.S. Chin, P. Neelakantan, H.P. Yoong, K.T.K. Teo, "Optimization of Fuzzy based MPPT in PV System for Rapidly Changing Solar Irradiance", *Transaction on Solar Energy and Planning*, 2011.
- [10] M. Braun, G. Arnold, and H. Laukamp, "Plugging into the zeitgeist," *IEEE Power Energy Mag.*, vol. 7, no. 3, pp. 63–76, 2009.
- [11] Yang, Tao (2013) Development of Dynamic Phasors for the modeling of aircraft electrical power systems. PhD thesis, University of Nottingham, chapter 2, pp. 45 -66.